J. Physiol. (1977), **270**, *pp.* 321–344
With 10 *text-figures*
Printed in Great Britain

QUANTITATIVE ANALYSIS OF THE VELOCITY CHARACTERISTICS OF OPTOKINETIC NYSTAGMUS AND OPTOKINETIC AFTER-NYSTAGMUS

BY BERNARD COHEN, VICTOR MATSUO AND THEODORE RAPHAN

From the Department of Neurology, Mount Sinai School of Medicine of the City University of New York, New York, N.Y. 10029, U.S.A.

(*Received 1 November 1976*)

SUMMARY

1. Velocity characteristics of optokinetic nystagmus (OKN) and optokinetic after-nystagmus (OKAN) induced by constant velocity full field rotation were studied in rhesus monkeys. A technique is described for estimating the dominant time constant of slow phase velocity curves and of monotonically changing data. Time constants obtained by this technique were used in formulating a model of the mechanism responsible for producing OKN and OKAN.

2. Slow phase velocity of optokinetic nystagmus in response to steps in stimulus velocity was shown to be composed of two components, a rapid rise, followed by a slower rise to a steady-state value. Peak values of OKN slow phase velocity increased linearly with increases in stimulus velocity to 180°/sec. Maximum slow phase eye velocities in the monkey are 2–3 times as great as in humans.

3. At the onset of OKAN, slow phase velocity falls by about 10–20%, followed by a slower decline to zero. Peak OKAN slow phase velocities were linearly related to optokinetic stimulus velocities up to 90–120°/sec. Above 120°/sec OKAN slow phase velocity saturated although OKN slow phase velocity continued to increase.

4. The charge and discharge characteristics of OKAN were studied. The OKAN mechanism charged in 5–10 sec and discharged over 20–60 sec in darkness. The time constants of decay in OKAN slow phase velocity decreased as stimulus velocities increased. They also decreased on repeated testing. In several monkeys there was a consistent difference in the rate of decay of OKAN slow phase velocity to the right and left.

5. Extended visual fixation discharged the activity responsible for producing OKAN. Short fixation times caused only a partial discharge

of the OKAN mechanism. Following brief periods of fixation, OKAN resumed but with depressed slow phase velocities.

6. A model based on a state realisation of a peak detector was formulated which approximately reproduces the salient characteristics of OKN and OKAN. This model predicts the three dominant characteristics of OKAN: (1) charge over 5–7 sec, (2) slow discharge in darkness, and (3) rapid discharge with visual fixation. With the addition of direct fast forward pathways, it also correctly predicts the rapid and slow rise in OKN. We postulate that OKAN is produced by a central integrator which is also active during OKN. Presumably this integrator acts to maximize velocities during OKN and to smooth and stabilize ocular following during movement of the visual surround.

INTRODUCTION

Optokinetic nystagmus (OKN) is nystagmus induced by continuous movement of the whole or a part of the visual field. In monkeys the eyes are powerfully driven by whole field rotation and the nystagmus lasts as long as the stimulus continues. Under this condition slow phase eye velocities are achieved which follow stimulus velocities into the saccadic range (Komatsuzaki, Harris, Alpert & Cohen, 1969). When the stimulus is terminated, if animals are in darkness, there is a persistent after-response, optokinetic after-nystagmus (OKAN). In the monkey, appreciable periods of OKAN regularly follow OKN provided the animal is alert, the stimulus is of adequate duration and visual fixation is prevented (Krieger & Bender, 1956; Komatsuzaki *et al.* 1969). There are generally two phases of OKAN. In the first phase the nystagmus is in the same direction as during OKN. This is often followed by a second phase which is oppositely directed (Aschan, Bergstedt & Stahle, 1956). Both OKN and OKAN are present in horizontal and vertical planes (Krieger & Bender, 1956) and are found in a wide range of species (Ter Braak, 1936; Rademaker & Ter Braak, 1948).

The significance of OKN is that it stabilizes the retinal image of a moving environment (Ter Braak, 1936). OKAN is noteworthy because it appears to compensate for vestibular after-responses (Ter Braak, 1936; Mowrer, 1937). In addition, OKAN is of interest because it is a motor response to a prolonged central excitatory state which is produced simply by viewing a moving visual field.

Although general characteristics of OKN and OKAN have been described, quantitative relationships between stimulus velocity and slow phase eye velocity have not been extensively studied, nor has the precise relationship between OKN and OKAN been elucidated. In this paper the

velocity characteristics of slow phases of OKN and OKAN induced by full field rotation are described. Only horizontal OKN and the first phase of OKAN are considered. A model was formulated from the data to predict characteristics of OKN and OKAN. The model suggests how the central mechanism which produces OKN and OKAN might be organized and gives a theoretical framework in which to study and understand the system performance.

METHODS

Five juvenile rhesus monkeys (*Macaca mulatta*) of 2–3 kg were used in this study. During testing, monkeys sat in a primate chair with head fixed. Amphetamine sulphate (0·5 mg/kg) was given 30 min before testing to maintain alertness. Horizontal and vertical movements of both eyes were recorded by electrooculography (EOG) using implanted Ag-AgCl electrodes (Bond & Ho, 1970). Drift rates of the implanted electrodes were negligible over 3–4 hr, the period of each experiment. The amplifiers had a passband of 0 –150 Hz. The EOG was differentiated by amplifiers with a 3 msec time constant and rectified to get the velocity of slow phases of nystagmus. Slow phase velocity was integrated to obtain time constants (see below). The EOG, its time derivatives and voltages representing stimulus parameters were recorded on paper and stored on FM magnetic tape. A general purpose digital computer was used to analyse the data and generate the graphs and model predictions.

OKN was induced by an internally lit, servo-controlled, rim-driven rotating drum, 90 cm in diameter and 60 cm high. It surrounded the animal and filled the field of vision. The drum wall was made of opalescent white plastic with 3° black stripes at each 45°. A mirror placed under the monkey's chin reflected stripes on the roof of the drum and extended stimulus movement to the lower portions of the visual field. Levels of illumination were in the photopic range.

Optokinetic stimuli consisted of constant velocity drum rotations. We refer to this type of optokinetic stimulation as full field or whole field rotation, since not only the stripes but the textured background contributed to the response. Velocities from 5 to 270°/sec were used to induce OKN, and were monitored by measuring the passage of drum stripes with a photocell. OKAN was recorded in total darkness after OKN had been induced.

To determine the relationship between the slow phase velocity of OKAN and stimulus duration, varying periods of optokinetic stimulation were given and peak OKAN velocity was measured. During these experiments the rotating drum was illuminated for variable periods. The rising and falling time constants of the light were approximately 20 msec. This was short enough to approximate a step in stimulus velocity.

Visual fixation of a stationary target has a strong suppressive effect on OKAN (Krieger & Bender, 1956; Takemori & Cohen, 1974*a*). The characteristics of this suppression were investigated by illuminating the stationary drum for short periods during OKAN. Slow phase velocities just before and after illumination were compared.

Eye movement recordings were normalized with respect to the velocity of slow phases of OKN recorded at 60°/sec. It was assumed that the gain of the optokinetic response

$$\frac{\text{Steady-state eye velocity}}{\text{Drum velocity}}$$

was approximately equal to 1 at 60°/sec (Komatusuzaki *et al.* 1969; Aschoff & Cohen, 1971). Calibrations were done just before each trial and were repeated after periods in darkness to control for gain changes in the EOG. Eye movements to the right are represented in the figures by upward trace deflexions.

Time constants

To obtain a simple piecewise linear model which would explain the operation of the system generating the slow phases of OKN and OKAN, exponential slow phase velocity profiles must be implicitly assumed. However, slow phase velocity profiles during OKAN may not be exponential due to nonlinearities in the system. Therefore standard techniques would not be suitable for estimating time constants of velocity declines. To overcome this difficulty a more general definition of time constant was established which gave a consistent description of the time domain behaviour of OKN and OKAN and could be related to measureable physical characteristics.

The dominant time constant for monotonically decreasing functions was defined as the time constant of an exponential having the same area under it as the physical data. A similar definition was used to find the dominant time constant of rising exponentials except that the steady-state level was considered to be the zero level. The mathematical formulation is as follows.

Consider an exponential function of the form

$$y = A \exp \frac{-(t-t_0)}{T}, \quad t \geqslant t_0,$$

where T is the time constant of the decline and A is the initial value. The area under the curve is the integral over the interval $[t_0, \infty)$ and is given by

$$\int_{t_0}^{\infty} y\,dt = \int_{t_0}^{\infty} A \exp \frac{-(t-t_0)}{T} dt = AT$$

therefore,

$$T = \frac{\int_{t_0}^{\infty} y\,dt}{A}.$$

This relationship can now be used to define the dominant time constant of any continuous function of time whose absolute value is monotonically decreasing and has finite area under it.

Definition

Let $f(t)$ be a real valued continuous function of time defined on the interval $[t_0, \infty)$ such that its absolute value is monotonically decreasing, its integral over the interval $[t_0, \infty)$ is finite, and its maximum value at $t = t_0$ is $f(t_0) = f_{max}$. The dominant time constant T is defined as

$$T = \frac{\int_{t_0}^{\infty} f(t)\,dt}{f_{max}}.$$

If $f(t)$ is a velocity function, as is the case in this study, then $\int_{t_0}^{\infty} f(t)\,dt$ has a ready physical interpretation as total eye deviation and f_{max} is the maximum velocity.

Therefore the definition adopted for the dominant time constant T of the primary OKAN response can be stated as follows:

$$T = \frac{\text{Total eye deviation during OKAN}}{\text{Peak velocity of OKAN}}.$$

Two examples of velocity declines during OKAN induced by stimulation at 60°/sec are shown in Fig. 1. Exponentials fitted to the velocity declines are shown by the dashed lines above the traces. The time constants were 16·2 and 5·3 sec for the decay in velocity of left and right nystagmus, respectively.

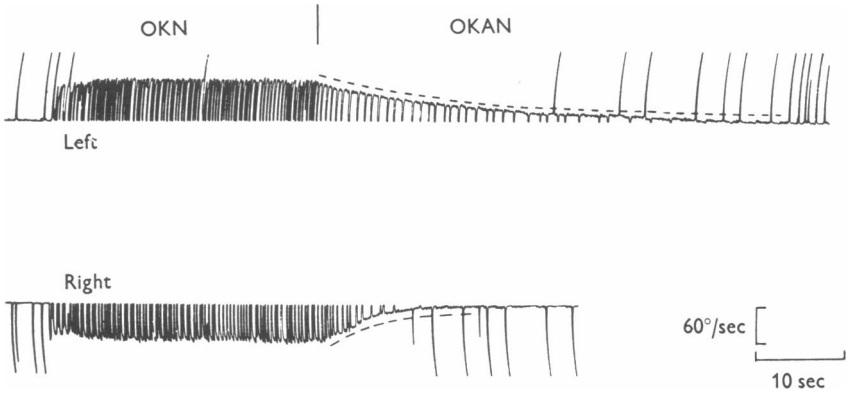

Fig. 1. Velocity of slow phases of OKN and OKAN induced by full field rotation at 60°/sec. Note the faster decline in slow phase velocity during right OKAN. The interrupted lines adjacent to the traces are the exponentials estimating the velocity declines during OKAN. They were translated by a small amount so that they would not be obscured by the data. The time constants of the declines were 16·2 and 5·3 sec for left and right OKAN, respectively.

RESULTS

OKN: Velocity traces during OKN and OKAN for step inputs of stimulus velocity between 29 and 180°/sec are shown in Fig. 2. In each instance, the velocity of the slow phases of OKN rises rapidly during the first few beats of nystagmus. The initial rise in velocity is followed by a more gradual rise to the steady-state value. A typical response is shown in Fig. 3*A*. The downward arrow indicates the rapid rise in OKN velocity and the bar, the approximate duration of the steady-state nystagmus. This response pattern was present in OKN induced by every stimulus velocity from 5 to 270°/sec.

To characterize the fast and gradual rises in slow phase velocity, pulses of optokinetic stimulation ranging from 0·1 to 10 sec were given at 45, 60 and 90°/sec. Peak slow phase velocity was measured and normalized with respect to stimulus velocity. Velocities reached during the initial rapid rise in OKN tended to have a constant relationship to the steady-

state value (Fig. 3*B*, *C*, *D*). In the animal which was most extensively studied, monkey 991, this ratio ranged from 0·55 to 0·65 for OKN induced by stimuli between 29 and 90°/sec. The gradual rise to a steady state was

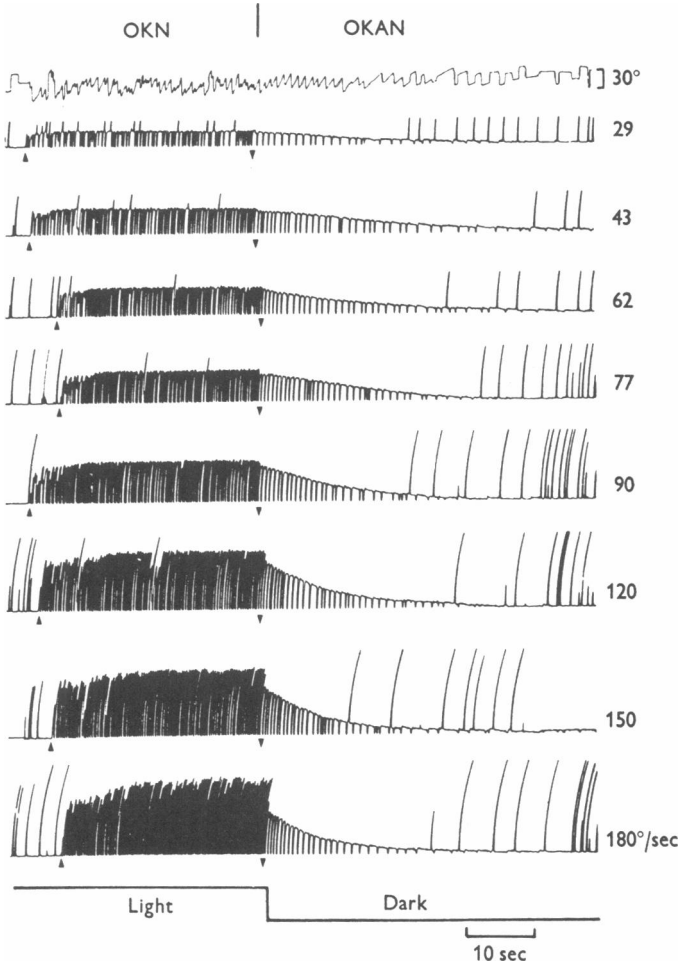

Fig. 2. Slow phase velocity of OKN and OKAN induced by full field rotations of 29 to 180°/sec. The horizontal EOG and slow phase velocity trace are both shown for the stimulus of 29°/sec. For other stimuli only the slow phase velocity trace is shown. The arrows show the onset and end of stimulation. During OKN there was an initial rapid rise in velocity followed by a slower rise to a steady state level. At the onset of OKAN there was an initial fall in slow phase velocity, followed by a slower decline to zero. The rate of decline during OKAN increased with increases in stimulus velocity. The calibration for the velocity traces is given by the amplitude of the steady-state OKN velocity which is assumed to be approximately equal to that of the stimulus velocity.

characterized by a dominant time constant determined using the technique described in the Methods section. For drum velocities of 45 and 60°/sec, time constants of the slow rise were approximately 2·6 and 3 sec (Fig. 3*B*, *C*). At 90°/sec, there was a small increase in the time constant to 3·3 sec (Fig. 3*D*). Above 90°/sec, time constants were more prolonged, being in the range of 5–7 sec.

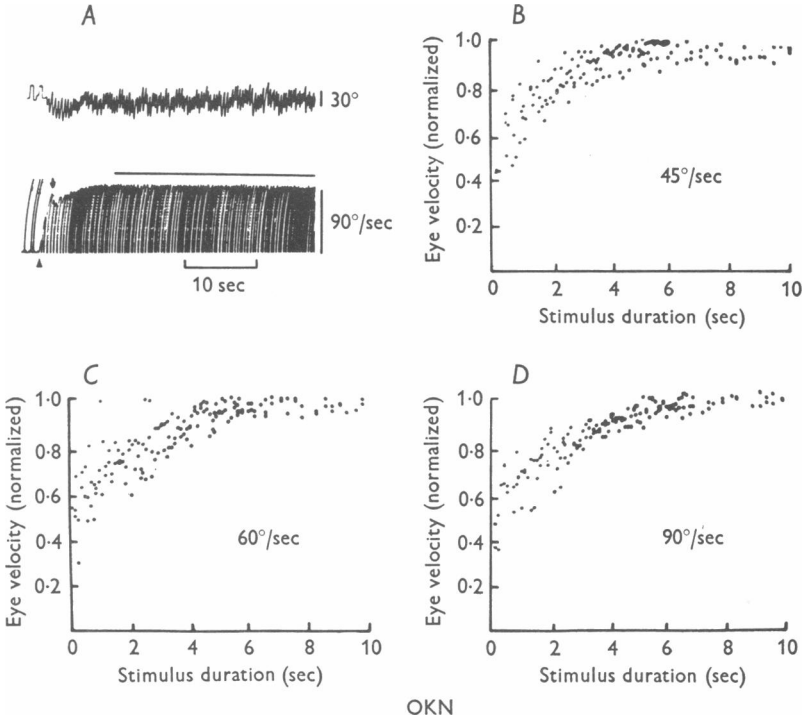

Fig. 3. *A*, typical example of rapid and slow rise characteristics of OKN. Stimulation velocity, 94°/sec. EOG, upper trace, and slow phase velocity, lower trace. The upward arrow marks the onset of stimulation, the downward arrow the rapid rise and the bar the steady-state velocity. *B–D*, slow-phase velocities induced by varying durations of stimulation from 0·1 to 10 sec. Stimulus velocities were 45 (*B*), 60 (*C*), and 90°/sec (*D*). In this and the subsequent graphs each dot represents the maximum slow phase velocity reached in a separate trial. Note that the fraction of steady-state velocity reached during the initial rapid rise was similar for 45, 60 and 90°/sec (*D*). Note also that the slow rise took somewhat longer at higher stimulus velocities. Time constants of the rise were 2·6, 3 and 3·3 sec respectively for *B–D*.

During continuous stimulation at velocities of 90°/sec and below, steady-state values of OKN slow phase velocity were maintained with little or no variation for long periods of time. Figs. 2, 29–90°/sec and 3*A* show the

type of steady-state response which could be elicited in monkey 991 for periods as long as 10–15 min. Variation in steady-state slow phase velocity progressively increased as the stimulus moved faster than 120°/sec (Fig. 2, 150 and 180°/sec).

OKN steady-state velocity increased with increase in drum velocity over a wide range. Fig. 4*A* shows slow phase eye velocities obtained in response to stimulation at 64 and 180°/sec. The steady-state velocity for

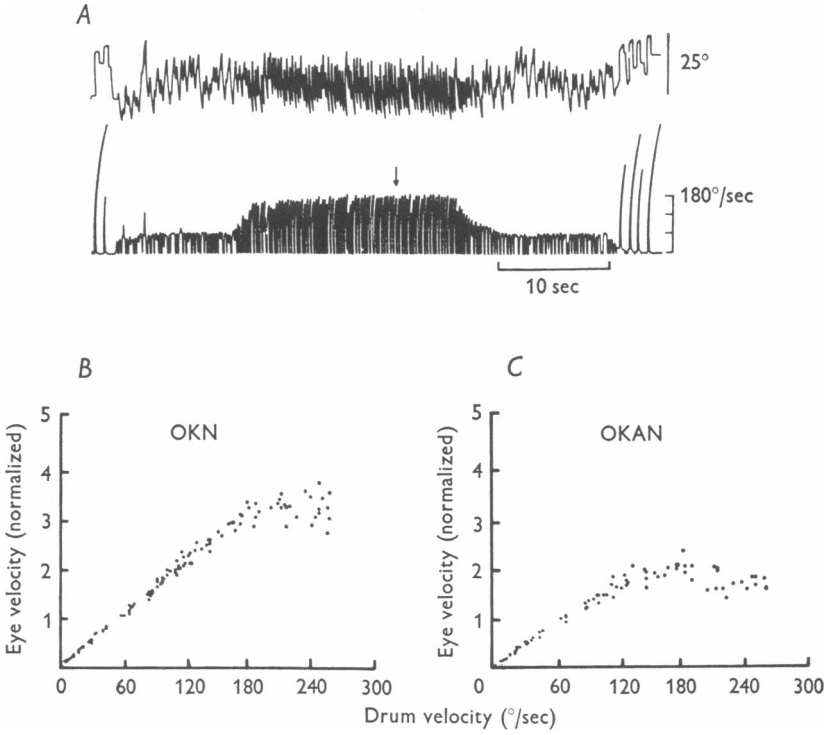

Fig. 4. *A*, OKN induced by stimuli of 64 and 180° sec. EOG, upper trace, and slow phase velocity, lower trace. Arrow marks onset of steady-state velocity for 180°/sec stimulus. *B*, slow phase velocities of OKN induced by stimuli from 5 to 270°/sec. Each dot represents the steady-state velocity attained in one trial. Velocities are normalized in relation to 60°/sec which is shown as 1 on the ordinate. Note that stimulation at 120°/sec induced eye velocities twice that at 60°/sec and 180°/sec three times the 60°/sec velocity. *C*, peak OKAN velocity induced by the same stimuli as in *B* and normalized in relation to the OKN velocity induced by 60°/sec. stimulation. Measurements were taken at the onset of OKAN just after the initial fall in velocity.

the 180°/sec stimulus, reached at about the downward arrow in Fig. 4*A*, was proportionally greater than the velocity for the 64°/sec stimulation. Similar experiments were performed with stimuli ranging from 5 to

270°/sec, using the eye velocity obtained for a 60°/sec stimulus as a normalization velocity. A graph of normalized slow phase eye velocity as a function of stimulus velocity (Fig. 4*B*) shows them to be linearly related up to a stimulus velocity of 180°/sec. Above 180°/sec slow phase velocities increased nonlinearly but monotonically, with the curve levelling at drum rotations of from 240 to 270°/sec.

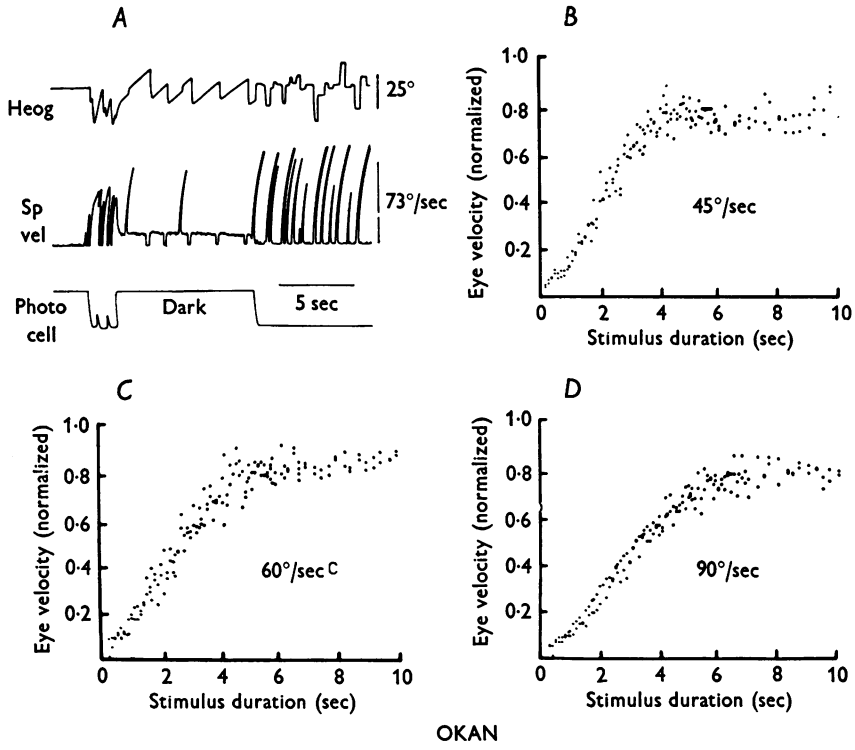

Fig. 5. Charge of OKAN mechanism by full field rotation. *A*, stimulation for a brief period (1·8 sec) at 73°/sec induced OKN and OKAN. The stationary OKN drum was lighted 10 sec after the onset of OKAN terminating the trial. Note the abrupt drop in slow phase velocity at the onset of OKAN. *B–D*, OKAN velocities attained after optokinetic stimulation of varying durations at 45, 60 and 90°/sec. Note the slower rise time for the charge in response to the faster stimuli.

OKAN: Typical examples of OKAN in response to different stimulus velocities are shown in Fig. 2. At the onset of OKAN slow phase velocity dropped rapidly within the first few beats. For stimuli of from 29 to 90°/sec, the fall in slow phase velocity was about 10–20%. This initial decline was followed by a more gradual decline in slow phase velocity approaching zero over 20–60 sec.

Slow phase velocity at the beginning of OKAN just after the rapid fall was a function of both the velocity and duration of the preceding optokinetic stimulus. As long as steady-state OKN had been reached, peak OKAN velocities increased proportionately with stimulus velocities up to 90–120°/sec (Fig. 4*C*). The slope of the increase in OKAN slow phase velocity was approximately 0·8 of the slope of the increase in OKN velocity (Fig. 4*B*). Above 90–120°/sec peak OKAN velocities saturated despite increases in drum and OKN slow phase velocity (Figs. 2, 150, 180°/sec, and 4*C*). This demonstrates that the mechanisms responsible for OKN and OKAN are not identical.

Charge characteristics of OKAN

For brief stimuli peak values of the slow phase velocity of OKAN could be considerably smaller than the OKAN velocities reached after steady-state OKN. An example is shown in Fig. 5*A*. The animal received a step of stimulus velocity of 73°/sec for 1·8 sec. At the start of OKAN, there was an initial drop in slow phase velocity of about 60%. This was much greater than the 10–20% drop in slow phase eye velocity after steady-state OKN had been reached (Fig. 2, 29–90°/sec).

The charge characteristics of the OKAN mechanism were determined by giving pulses of full field rotation for periods of 0·1–10 sec at velocities of 45, 60 and 90°/sec. Peak OKAN velocity was normalized with respect to stimulus velocity and plotted as a function of stimulus duration. The velocity increased steadily with increases in the duration of stimulation (Fig. 5*B-D*). The time constants of rise ranged from 2·6 to 3·3 sec and increased slightly with increases in stimulus velocity. At each stimulus velocity the time constants were approximately the same as those of the slow rise in velocity during OKN (Fig. 3*B-D*). This is shown in Fig. 6 in which data from charge experiments of OKN (*A*) and OKAN (*B*) induced by the same stimulus (60°/sec) were well fitted by exponentials with the same time constant.

Discharge characteristics of OKAN in darkness

After the initial rapid fall at the onset of OKAN, slow phase velocity in darkness declined slowly but continuously. The decline appeared relatively linear at lower stimulus velocities (Fig. 2, 29 and 43°/sec) and was close to an exponential decay at higher stimulus velocities (Fig. 1; Fig. 2, 62–180°/sec). Time constants of the declines decreased with increases in stimulus velocity up to about 90°/sec (Figs. 2 and 7). Similar data have been reported by Buettner, Waespe & Henn (1976). Of the five monkeys used in this study the rate of decay in OKAN slow phase velocity was symmetrical in 3. In two other monkeys, however, there was a con-

sistent difference in the time constants of slow phase velocity declines for rightward and leftward beating nystagmus. An example is shown in Fig. 1. In this monkey (991), time constants initially ranged from 18 to 24 sec for left OKAN and from 10 to 14 sec for right OKAN. With repeated

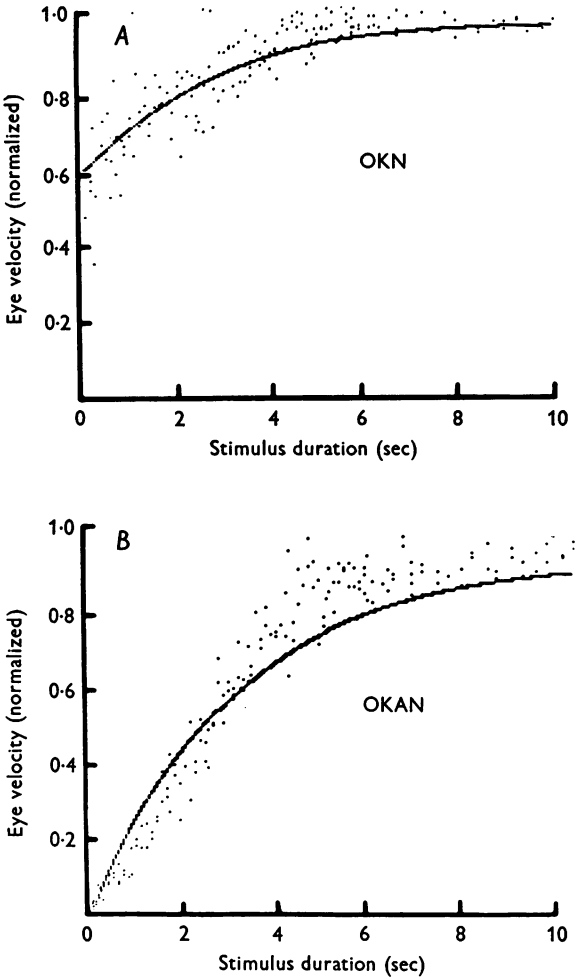

Fig. 6. Approximation of data from slow rise of OKN (*A*) and charge of OKAN mechanism (*B*) by exponentials with the same time constant (3 sec). The stimulus was 60°/sec for both groups of data. Dots are data and continuous lines the exponential fits to the data.

testing over a 6 month period the time constants became shorter, ranging from 9 to 20 sec and from 5 to 10 sec for left and right OKAN, respectively (Fig. 7*A*). As testing continued, time constants fell further, particularly

for velocities less than 90°/sec (Fig. 7*B*). However, the difference between the two sides was maintained, with OKAN being shorter for right and left nystagmus.

Discharge characteristics of OKAN in light: effects of fixation

If animals are allowed to fixate at the end of OKN, OKAN is brief (Krieger & Bender, 1956) (Fig. 8*A*). During visual fixation the eyes move in the slow phase direction (Fig. 8) (Takemori & Cohen, 1974*a*), and slow phase velocity drops abruptly. If short periods of visual fixation were allowed during OKAN, nystagmus resumed when animals were again in darkness (Fig. 8*B*). The velocity of the slow phase of this nystagmus (downward arrow) was less than the velocity that would have occurred without fixation. This demonstrates that the mechanism responsible for OKAN had lost activity during the short period of fixation.

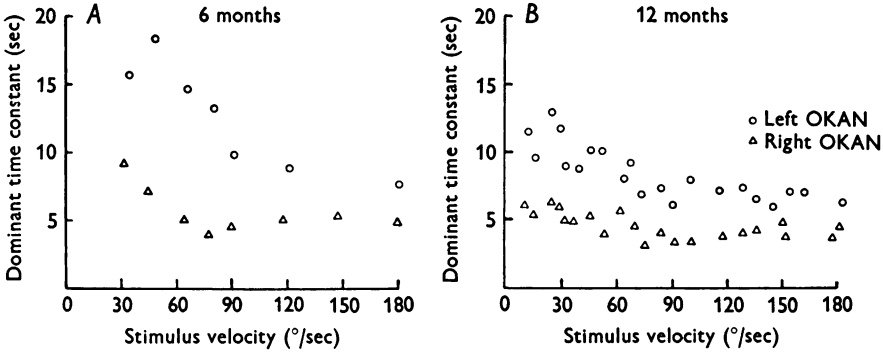

Fig. 7. Time constants of velocity declines in OKAN of monkey 991, 6 (*A*) and 12 (*B*) months after the onset of testing. Time constants of left OKAN are shown by circles and right OKAN by triangles. The time constants tended to be shorter for higher stimulus velocities and longer for left than right OKAN.

The effect of visual fixation on subsequent OKAN eye velocity was investigated using fixation durations from 0·1 to 4·0 sec. Fig. 8*C* shows the function obtained when the ratio of OKAN recovery velocity to the eye velocity immediately prior to fixation was plotted against fixation duration. The data can be described by a monotonically decreasing function which was zero for fixation durations of 3 sec or longer. The time constants of the decline due to fixation ranged from 1 to 1·4 sec and were similar for all velocities of stimulation. This was about one third to one half of the rising time constant for OKAN. Differences in the time course of the charge of the OKAN mechanism and of its discharge in light are shown in Fig. 8*D*.

The asymmetry in the time constants of velocity decreases of OKAN in darkness in monkey 991 (Figs. 1 and 7) had no discernible effect on discharge characteristics of OKAN in light. Similar times for discharge of OKAN in light were observed in other monkeys. In each animal the time course of the charge of OKAN was different from the time course of the discharge of OKAN either in darkness or during fixation.

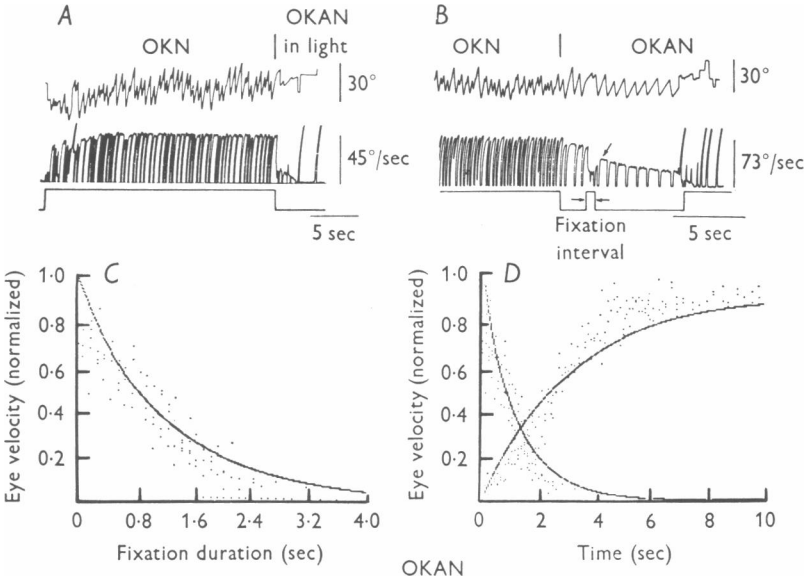

Fig. 8. *A*, OKN and OKAN recorded in light. EOG, top trace; slow phase velocity, middle trace; duration of stimulus, bottom trace. The animal was in light for the duration of the recording in *A*. Note the brief duration of OKAN and the rapid decline of slow phase velocity at the end of stimulation. *B*, OKN followed by OKAN. The OKAN was terminated after 10 sec. The bottom trace shows the occurrence of light and darkness. There was a rapid decline in slow phase velocity during fixation, and recovery after fixation (arrow). The post-fixation recovery level was lower than would have occurred had fixation not been given. *C*, post-fixation OKAN velocity normalized with respect to prefixation velocity (ordinate) as a function of fixation duration. OKAN was lost after fixation durations of about 3 sec. *D*, comparison of the time course of loss of OKAN activity due to fixation (falling data) to the time course of charge of OKAN mechanism (rising data). The discharge of activity was about twice as fast as the charge.

Model formulation

A mathematical model was formulated to predict and explain the neural mechanism responsible for producing OKN and OKAN. Assumptions on which the model are based will be considered first.

The persistence of nystagmus in darkness after OKN indicates that the

nervous system stores activity during full field rotation which is later used to drive the eyes during OKAN. Storage is assumed to be due to the charge of a central integrator or integrators (Collewijn, 1972*a*, *b*).

The charge experiments of Fig. 5 indicate that the stored activity responsible for OKAN is not accumulated instantaneously, but builds up over a finite time which in several monkeys was 5–15 sec. Discharge of stored activity in light is faster than in darkness but also takes several seconds (Fig. 8*C*). The difference in discharge time of OKAN in light and darkness suggests that some parameters vary non-linearly when going from light to dark. The time constants of charge and discharge in light and darkness were different from each other and are taken as independent parameters of the system.

The time course of the discharge of activity responsible for OKAN in darkness was different in several monkeys for nystagmus to the right and to the left. This difference is interpreted to mean that separate storage mechanisms were responsible for producing OKAN in the two directions.

OKN was shown to be separable into two components, one rising rapidly, and another rising more slowly (Figs. 2, 3). These two components were present in OKN induced at all stimulus velocities, suggesting that OKN was similarly generated regardless of stimulus speed. Presumably the subsystems responsible for producing these two components work synergistically to give the steady-state OKN response. OKAN, on the other hand, appears to have only a slow component.

The time constants of the slow rise in velocity during the build-up of OKN to steady state levels were approximately equal to the time constants of charge of slow phase velocity of OKAN (Fig. 6*A*, *B*). In addition, OKAN slow phase velocity did not attain its peak value until steady-state OKN had been reached. These findings suggest that the mechanisms responsible for the gradual rise in OKN slow phase velocity and for the accumulation of activity responsible for OKAN are the same. The rapid component of OKN is assumed to be due to the presence of direct pathways from the visual system which bypass the storage mechanism and are gradually inactivated when OKAN begins. Evidence for inactivation is the small drop in eye velocity at the onset of OKAN after steady-state OKN is reached as compared to the large drop in OKAN velocity after shorter periods of stimulation (Fig. 5*A*).

Mathematical modelling of OKN and OKAN generation

Phenomenological aspects of OKN and OKAN were consolidated in a model which approximately predicts their characteristics and give a theoretical framework for understanding the system operation. The most important property which characterizes OKAN is the difference in time

constants of its charge (Fig. 5) and of its discharge in darkness (Figs. 1 and 2). This property is characteristic of non-linear system, since if the system were linear, the rise and fall times would have been the same.

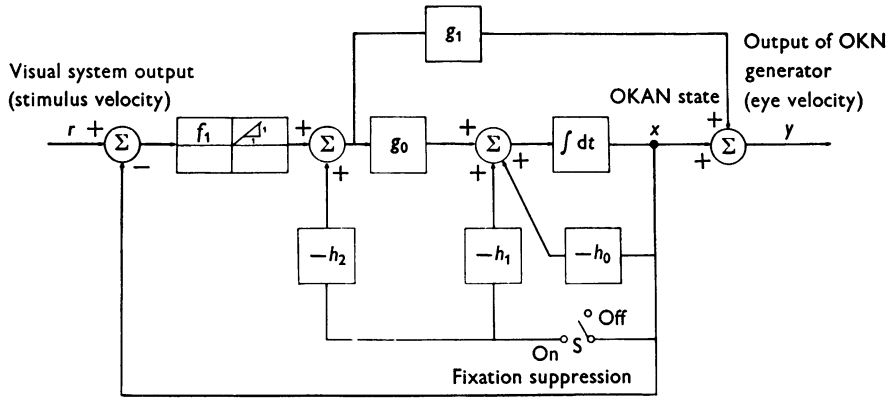

Fig. 9. Model of neural mechanism responsible for producing OKN and OKAN in one direction. Parameter values used in the model are $g_0 = 0{\cdot}25$; $g_1 = 0{\cdot}6$; $h_0 = 0{\cdot}085$; $h_1 = 0{\cdot}7$; $h_2 = 1{\cdot}2$. Rising time constant, $T_r = 3$ sec; visual suppression time constant, $T_1 = 1$ sec; time constant in darkness $T_d = 12$ sec.

This non-linear characteristic was modelled using peak detection theory (Javid & Brenner, 1963). In order to relate model variables to the nervous system, a state realization of a model containing a peak detector was developed (Zadeh & Desoer, 1963). This model is shown in Fig. 9. It has two sides, only one of which is presented for simplicity. The mathematical analysis of this model appears in the Appendix. The input in this system is an internal stimulus velocity signal r which is presumably obtained by efference copy adding to a retinal error signal (Young, 1971; Koerner & Schiller, 1972; Yasui, 1974; Yasui & Young, 1975). During stimulation r is assumed to be equal to drum velocity. In darkness $r = 0$ since retinal error is zero and the efference feed-back is assumed to be inactivated (Yasui, 1974; Yasui & Young, 1975). The non-linear element f_1 allows transmission in only one direction separating the integrators on the two sides. The forward gain parameters g_0 and g_1, and the feed-back parameters h_0, h_1 and h_2 determine the rise and fall characteristics of the system. There is a saturating integrator $\int dt$ and a direct forward pathway g_1 which bypasses the integrating circuit. Both the integrating circuit and the direct pathway sum to give the velocity signal y which drives the eyes.

When the OKN velocity input is greater than the state of the integrator, a signal is transmitted through the gain element g_0 which charges the

integrator. Parameters g_0 and h_0 determine the charge characteristics of the OKAN state, the time constant of the rise T_r being

$$T_r = \frac{1}{g_0 + h_0}.$$

These parameters also determine the extent to which the integrator can be charged. It is predicted that the maximum value of the state of the OKAN generator x_{max} is always less than that of the OKN velocity signal.

$$x_{max} = \frac{g_0}{g_0 + h_0}. \text{ Input velocity.}$$

This would explain the initial decline in slow phase velocity at the onset of OKAN shown in Fig. 2.

While the integrator is being charged, an OKN velocity signal is also transmitted through a direct forward pathway g_1. As the integrator charges, the signal which drives the direct forward pathway diminishes because of the negative feed-back from the OKAN state which subtracts from the stimulus velocity signal. When the integrator is completely charged, it is predominantly responsible for producing the velocity signal driving the eyes. At the end of stimulation, the internal velocity signal drops to zero ($r = 0$), and the negative signal feeding back from the OKAN state cannot be transmitted through the non-linear element f_1. Consequently the integrator discharges with its own characteristic time constant

$$T_d = \frac{1}{h_0}.$$

Visual fixation in the model is accounted for by the switch, S, and the additional feed-back elements, h_1 and h_2. In darkness, the switch is open and the OKAN integrator discharges with a long time constant, as described. However, when fixation is permitted the switch is closed and eye velocity drops rapidly due to the direct feedback around the integrator through elements h_2 and g_1. The OKAN integrator itself discharges in light with a time constant

$$T_1 = \frac{1}{h_0 + h_1 + h_2 g_0}.$$

Since $h_0 + h_1 + h_2 g_0$ is greater than h_0, the time constant of the discharge during fixation suppression T_1 is smaller than the time constant of the decline of OKAN in darkness T_d. Since the rising time constant T_r is $1/(h_0 + g_0)$, the charge and discharge of the OKAN integrator are different if $h_1 + h_2 g_0$ is not equal to g_0.

Fig. 10*A* shows the model response to a step input. The solid rising line represents the rise in OKN slow phase velocity and the dashed line the

charge of the OKAN state x. The rising phase of the curves is similar to the data shown in Figs. 3, 5 and 6.

The model predicts an incomplete charge for stimulus durations shorter than the charging time $T_r = 1/(g_0+h_0)$. The predicted discharge of the model in darkness after varying durations of stimulation is also shown in Fig. 10*A*. It can be compared to the actual declines of OKAN velocities

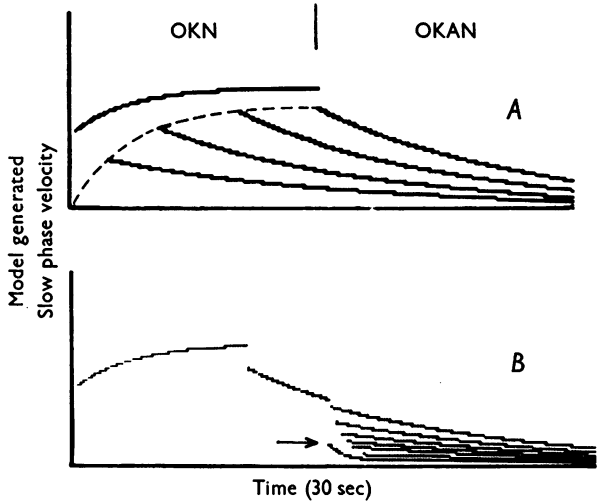

Fig. 10. *A*, curves generated by OKN-OKAN model. The input was a step in stimulus velocity of 60°/sec. Slow phase velocity during OKN increases along continuous rising line. The OKAN mechanism charges along dashed rising line. The falling lines show the decay of OKAN slow phase velocity after stimuli of varying durations. The initial drop in velocity at the onset of OKAN can be compared to the data of Figs. 2, 3 and 5. *B*, curves of discharge of OKAN mechanism caused by varying periods of fixation. The predicted values can be compared to the data of Fig. 8 *B* and *C*.

shown in Figs. 2 and 5*A*. Because the eye velocity signal shown in the model is processed through a neural integrator and plant (Robinson, 1964, 1965), there may be slight differences between actual eye velocity and that predicted by the model. However, this neural integrator is almost ideal, being able to hold the eyes in fixation for seconds or minutes and the plant dynamics would not significantly alter the response. Thus they can be neglected and the curves should be nearly identical.

A partial discharge of activity in the OKAN state caused by closing the visual fixation switch S is shown in Fig. 10*B*. The lowermost solid line, marked by the arrow, demonstrates predicted eye velocity of OKAN during fixation in light, and the intermediate lines the OKAN after shorter periods of fixation. There is an abrupt drop in velocity during the period

of switch closure followed by a slow decline toward zero once the fixation switch has been opened. This can be compared to Fig. 8*A*, *B*, which show the decline of slow phase velocity of a monkey in response to similar periods of fixation. Fixation in this model has been represented by a simple switch. Higher functions which compare stimulus velocity to the OKAN state and activate the suppression mechanism are necessary to correctly model the response to pulse steps and sinusoids. These higher functions have been developed but are omitted for simplicity because we have only considered the fixation mechanism for a stationary target.

DISCUSSION

The model is a first order approximation of a complex system and some of the data would be more exactly described by a higher order non-linear system. The usefulness of a simple approach is that the charge and discharge of activity and the effects of visual fixation can be described by single numbers, facilitating comparison of observed with predicted results. Despite its simplicity the model closely predicts OKN and OKAN of the alert monkey for step inputs in velocity of a full field stimulus. According to the model OKAN is produced by a subset of the system producing OKN. OKN is initially mediated through direct pathways from the visual system which drive the eyes to only a fraction of the stimulus velocity. As the stimulus and OKN continue, slower pathways are recruited permitting the velocity of the eyes to approximate the stimulus velocity more closely. Once the slower pathways are excited, the direct pathways gradually become inactive. Consequently, they contribute relatively little to the steady-state response for velocities up to 90–120°/sec. Above this level the slower pathways are saturated and the faster pathways are recruited as needed up to 180°/sec.

The nature and location of the pathways mediating the rapid component of OKN have yet to be determined. Features of the slow component, i.e. storage of activity as well as the characteristic charge and discharge times suggest that it is produced by a central integrator. The presence of an integrator in the mechanism producing OKN was previously inferred in the rabbit by Collewijn (1972*b*). It has generally been assumed that the functional significance of OKN is to stabilize a moving environment on the retina (Ter Braak, 1936). An integrator with a long time constant would contribute to the ocular response by stabilizing slow phase velocity, thereby reducing its variation. In addition it would make following at higher velocities possible since activity in direct pathways could add to that from the integrators to produce a faster combined response. The integrators saturate at levels that are well below the velocity of maximum

OKN following. Above the saturation level, i.e. at stimulus velocities greater than 90–120°/sec, OKN became increasingly irregular suggesting a greater contribution of the direct pathways to the over-all response.

It was of interest that monkeys could have proportional increases in slow phase eye velocity along with stimulus velocities of up to 180°/sec. Considering the gain of the OKN response to full field rotation to be close to 1, this is considerably faster than has been reported before and is about 2–3 times as fast as has been found in humans (Grüttner, 1939; Mackensen & Wiegmann, 1959). Careful attention to filling the entire visual field, particularly the lower portions, helped raise the maximum values attained.

Based on the differences in velocity declines during OKAN to the right and left, it is postulated that two integrators subserve nystagmus in the horizontal plane. These two integrators appear to be decoupled from each other and can have separate characteristic time constants. In the model different values of the parameter h_0 on the two sides would produce directional asymmetry. The shorter time constants of OKAN declines in darkness which were found at higher velocities and after repeated testing (Fig. 7) would also be produced by varying the value of h_0.

From the data incorporated in the model we infer that the integrators can only be charged to about 0·8 of stimulus velocity and that the direct forward pathways have a gain of 0·6 (Fig. 3*B–D*). Thus in the steady-state the direct pathways would contribute 12% [0·6(1 − 0·8)] and the OKAN state 80% of stimulus velocity. The sum of these, which determines OKN eye velocity would not be more than about 92% of the stimulus velocity. We have previously assumed that during full field rotation the velocity of slow phases of OKN in the monkey closely matches stimulus velocity up to 75–90°/sec. According to the model, this may overestimate slow phase velocity by about 8–10%. Alternatively, however, eye velocities could match stimulus velocities if the parameter g_1 were to be adapted during stimulation so that the overall gain of the OKN response would be equal to 1 in the steady-state. There is evidence that the central oculomotor system is capable of such adaptive behaviour both on a short-term (Gonshor & Melvill-Jones, 1976*a*) and long-term basis (Gonshor & Melvill-Jones, 1976*b*; Miles & Fuller, 1975; Ito, Shiida, Yagi & Yamamoto, 1974).

Brandt & Dichgans (1972) have shown that circular vection, a sense of self rotation, is closely associated with OKAN. The charge times (5–6 sec and discharge times (20–30 sec) of both OKAN and circular vection are comparable, and they both saturate at about 120°/sec (Brandt, Dichgans & Koenig, 1973). An explanation for these similarities is that circular vection is the result of monitoring activity in integrators which are associated with OKN and OKAN. Although these integrators seem related

to the feeling of self rotation, they could not be solely responsible for it. If the central and peripheral visual fields are moving in opposite directions, the sensation of movement is related to the peripheral stimulus, but OKAN is in the direction of OKN induced by the central visual field (Brandt, Dichgans & Büchele, 1974).

The integrators responsible for OKAN appear to be closely related to the vestibular system (Takemori, 1974; Cohen, 1974). OKAN is lost after bilateral labyrinthectomy (Uemura & Cohen, 1973; Cohen, Uemura & Takemori, 1973; Zee, Yee & Robinson, 1976) and is strongly affected by lesions of the ventral part of the lateral vestibular nucleus, and the medullary reticular formation in the region of the prepositus nucleus (Uemura & Cohen, 1973, 1975). In addition, activity of neurones in the vestibular nuclei closely parallels slow phase velocity during OKAN (Waespe & Henn, 1976).

Circuitry through the flocculus is probably responsible for the discharge of activity in the integrators during visual fixation (Maekawa & Simpson, 1973; Takemori & Cohen, 1974*b*; Lisberger & Fuchs, 1974). The cerebellum may also be responsible for adapting the various gain parameters which cause changes in time constants of OKAN at different velocities and after repeated testing (Ito *et al.* 1974; Robinson, 1975). However, the OKN and OKAN integrators could not be located in the flocculus nor be entirely dependent upon it since OKAN can be induced after bilateral flocculectomy (Takemori & Cohen, 1974*b*).

The loss of OKAN after bilateral labyrinthectomy suggests that the integrators which generate OKAN and the slow rise in OKN had become inactivated. Presumably, in such animals only the direct or fast forward pathways would be active during OKN. This would lead to the following consequences: (1) there would be only a rapid and not a slow rise in OKN, (2) the steady-state response would be more irregular, (3) OKN should saturate at lower velocities, probably at about 60–80°/sec (OKN saturation velocity-OKAN saturation velocity), (4) at lower stimulus velocities the relationship between drum and slow phase velocity would be expected to be about 0·6, the gain of the direct forward pathways.

Previously reported data on changes in OKN and OKAN after bilateral labyrinthectomy agree with these predictions. A normal monkey recorded before labyrinthectomy had both a slow and rapid rise in slow phase velocity in OKN, followed by typical OKAN. After bilateral labyrinthectomy there was only a rapid rise in OKN with no slow rise to a steady-state level (Fig. 8*E-H* of Uemura & Cohen, 1973, p. 16). OKN was irregular and there was no OKAN. The velocity of OKN was about two thirds of that recorded before operation and the animal could not follow at stimulus velocities faster than about 60°/sec. Findings were

similar in another monkey after bilateral labyrinthectomy (Fig. 2 of Cohen *et al.* 1973, p. 90). For 3–6 months after operation OKN slow phase velocity saturated at about 60°/sec, although it later recovered. Theoretically, recovery was due to adapted gain of the direct forward pathways, g_1. In other animals the failure to follow faster than 60–70°/sec during OKN after labyrinthectomy was permanent. Thus, the model fits the available data and provides a theoretical basis for understanding the behaviour of the central mechanism responsible for OKN and OKAN under normal and some pathological conditions.

Supported by N.I.H. Research Grant NINCDS 00294 and CUNY Research Faculty Award no. 11058. Theodore Raphan was supported by NINCDS Fellowship NS 052970. We thank Volker Henn for his help in some of the experiments and Valerie Josephson for assistance.

APPENDIX

Mathematical analysis of model

The mathematical state equation which describes the behaviour of the system shown in Fig. 9 is

$$\left.\begin{aligned} \dot{x} &= -h_0 x - h_1 x S + g_0 (r-x)\, U\,(r-x) - h_2 g_0 x S, \\ y &= x - g_1 h_2 x S + g_1 (r-x)\, U\,(r-x), \end{aligned}\right\} \tag{1}$$

where U is the Heaviside unit function or step, i.e.

$U(z) = \left\{\begin{matrix} 1 & z>0, \\ 0 & z<0, \end{matrix}\right\}$, r is the input, S is the fixation suppression factor such that $S = 0$ when there is no fixation and $S = 1$ when fixating. The state of the OKAN generator, x, is the signal driving a neural integrator during OKAN. In the usual experimental paradigm a step in velocity is applied (drum spinning at constant velocity). Therefore, let the input be a step in velocity, i.e. $r = VU(t)$, whose magnitude is V. The solution may be broken into various parts and will be derived in turn. For $r > x$ and $S = 0$, the state equation is

$$\left.\begin{aligned} \dot{x} &= -(h_0+g_0)x + g_0 V, \\ y &= (1-g_1)x + g_1 V. \end{aligned}\right\} \tag{2}$$

The solution to this differential equation is a rising exponential given by

$$\left.\begin{aligned} x(t) &= \frac{g_0}{h_0+g_0} V(1-\exp\{-(h_0+g_0)t\}, \\ y(t) &= g_1 V + (1-g_1)\frac{g_0}{h_0+g_0} V(1-\exp\{-(h_0+g_0)t\}), \end{aligned}\right\} \quad 0 < t \leqslant T_s \tag{3}$$

where T_s is the time of the driving OKN stimulus. At $t = T_s$

$$\left.\begin{aligned} x(T_s) &= \frac{g_0}{h_0+g_0} V(1-\exp\{-(h_0+g_0)T_s\}) \\ y(T_s) &= g_1 V + \frac{(1-g_1)g_0}{h_0+g_0} V(1-\exp\{-(h_0+g_0)T_s\}). \end{aligned}\right\} \tag{4}$$

If at $t = T_s$ the input is set to zero (lights are extinguished, $S = 0$), the differential equation describing this system is

$$\left.\begin{aligned} \dot{x} &= -h_0 x, \\ y &= x. \end{aligned}\right\} \tag{5}$$

The solution to this equation is an exponential decay beginning at $t = T_s$ with the initial value $x_s = x(T_s)$.

$$\left.\begin{aligned} x(t) &= x_s \exp -h_0(t-T_s), \\ y(t) &= x(t), \end{aligned}\right\} \quad t > T_s. \tag{6}$$

Eqns. (3) and (6) approximately describe the characteristics of OKAN generation. With the addition of switch, S, and the feed-back h_1 and h_2, the fixation suppression mechanism can be also modelled. If it is now assumed that at $t = T_L$ a light pulse is given with a duration D_L (suppression time) then the state equation describing the behaviour while fixating is:

$$\left.\begin{aligned} \dot{x} &= -(h_0+h_1+h_2g_0)x, \\ y &= (1-g_1h_2)x. \end{aligned}\right\} \tag{7}$$

The solution for the interval is

$$\left.\begin{aligned} x(t) &= x_{BL} \exp\{-(h_0+h_1+h_2g_0)(t-T_L)\}, \\ y(t) &= (1-g_1h_2)x_{BL} \exp\{-(h_0+h_1+h_2g_0)(t-T_L)\}, \end{aligned}\right\} \quad T_L < t \leqslant T_L + D_L \tag{8}$$

where x_{BL} is the state of the integrator just prior to the fixation. At the end of the fixation period, the system is again described by eqn. (5) with a different starting state and starting time. The solution is given by

$$\left.\begin{aligned} x(t) &= x_{AL} \exp\{-h_0(t-T_L-D_L)\}, \\ y(t) &= x_{AL} \exp\{-h_0(t-T_L-D_L)\}, \end{aligned}\right\} \quad t > T_L + D_L, \tag{9}$$

where

$$x_{AL} = x_{BL} \exp -\{(h_0+h_1+h_2g_0)D_L\}. \tag{10}$$

Eqns. (3), (4), (6), (8), (9) and (10) can be used to compare the experimental and modelled OKN and OKAN responses.

REFERENCES

ASCHAN, G., BERGSTEDT, M. & STAHLE, J. (1956). Nystagmography. *Acta oto-lar.* suppl. 129, 1–103.

ASCHOFF, J. C. & COHEN, B. (1971). Changes in saccadic eye movements produced by cerebellar cortical lesions. *Expl Neurol.* **32**, 123–133.

BOND, H. W. & HO, P. (1970). Solid miniature silver-silver chloride electrodes for chronic implantation. *Electroenceph clin. Neurophysiol.* **28**, 206–208.

BRANDT, T. & DICHGANS, J. (1972). Circularvektion, optische Pseudocoriolis-Effekte und optokinetischer Nachnystagmus. *Albrecht v Graefes Arch. Ophthal.* **184**, 42–57.

BRANDT, T., DICHGANS, J. & BUCHELE, W. (1974). Motion habituation: Inverted self motion perception and optokinetic after-nystagmus. *Expl Brain Res.* **21**, 337–352.

BRANDT, T., DICHGANS, J. & KOENIG, E. (1973). Differential effects of central versus peripheral vision on egocentric and exocentric motion perception. *Expl Brain Res.* **16**, 476–491.

BUETTNER, U., WAESPE, W. & HENN, V. (1976). Duration and direction of optokinetic after-nystagmus as a function of stimulus exposure time in the monkey. *Arch. Psychiat. NervKrankh.* **222**, 281–291.

COHEN, B. (1974). The vestibulo-ocular reflex arc. In *Handbook of Sensory Physiology*, vol. 6, ed. KORNHUBER, H. H., pp. 477–540. Munich: Bergman.

COHEN, B., UEMURA, T. & TAKEMORI, S. (1973). Effects of labyrinthectomy on optokinetic nystagmus (OKN) and optokinetic after-nystagmus (OKAN). *Equil. Res.* **3**, 88–93.

COLLEWIJN, H. (1972*a*). Latency and gain of the rabbit's optokinetic reactions to small movements. *Brain Res.* **36**, 59–70.

COLLEWIJN, H. (1972*b*). An analog model of the rabbit's optokinetic system. *Brain Res.* **36**, 71–88.

GONSHOR, A. & MELVILLE-JONES, G. (1976*a*). Extreme vestibulo-ocular adaption induced by prolonged optical reversal of vision. *J. Physiol.* **256**, 381–414.

GONSHOR, A. & MELVILL-JONES, G. (1976*b*). Short-term adaptive changes in the human vestibulo-ocular reflex arc. *J. Physiol.* **256**, 361–379.

GRÜTTNER, R. (1939). Experimentelle Untersuchungen uber den opto-kinetischen Nystagmus. *Z. Sinnesphysiol.* **68**, 1–48.

ITO, M., SHIIDA, T. YAGI, N. & YAMAMOTO, M. (1974). Visual influence on rabbit horizontal vestibulo-ocular reflex presumably effected via the cerebellar flocculus. *Brain Res.* **65**, 170–174.

JAVID, M. & BRENNER, E. (1963). *Analysis, Transmission and Filtering of Signals*, p. 180. New York: McGraw Hill.

KOERNER, F. & SCHILLER, P. H. (1972). The optokinetic response under open and closed loop conditions in the monkey. *Expl Brain Res.* **14**, 318–330.

KOMATSUZAKI, A., HARRIS, H. E., ALPERT, J. & COHEN, B. (1969). Horizontal nystagmus of rhesus monkeys. *Acta oto-lar.* **67**, 535–551.

KRIEGER, H. P. & BENDER, M. B. (1956). Optokinetic after-nystagmus in the monkey. *Electroenceph clin. Neurophysiol.* **8**, 97–106.

LISBERGER, S. G. & FUCHS, A. F. (1974). Response of flocculus Purkinje cells to adequate vestibular stimulation in the alert monkey: fixation vs. compensatory eye movements. *Brain Res.* **69**, 347–353.

MACKENSEN, G. & WIEGMANN, O. (1959). Untersuchungen zur Physiologie des optokinetischen Nachnystagmus *Albrecht v Graefes Arch. Ophthal.* **160**, 497–509.

MAEKAWA, K. & SIMPSON, J. I. (1973). Climbing fiber responses evoked in vestibulocerebellum of rabbit from visual system. *J. Neurophysiol.* **36**, 649–666.

MILES, F. A. & FULLER, J. H. (1974). Adaptive plasticity in the vestibulo-ocular responses of the rhesus monkey. *Brain Res.* **80**, 512–516.

MOWRER, O. H. (1937). The influence of vision during bodily rotation upon the duration of post-rotational vestibular nystagmus. *Acta oto-lar.* **25**, 351–364.

RADEMAKER, G. G. J. & TER BRAAK, J. W. G. (1948). On the central mechanism of some optic reactions. *Brain* **71**, 48–76.

ROBINSON, D. A. (1964). The mechanics of human saccadic eye movement. *J. Physiol.* **174**, 245–264.

ROBINSON, D. A. (1965). The mechanics of human smooth pursuit eye movement. *J. Physiol.* **180**, 569–591.

ROBINSON, D. A. (1975). Oculomotor control signals. In *Basic Mechanisms of Ocular Motility and Their Clinical Applications*, ed. LENNERSTRAND, G. & BACH-Y-RITA, P., pp. 337–374. Oxford and New York: Pergamon.

TAKEMORI, S. (1974). The similarities of optokinetic after-nystagmus to the vestibular nystagmus. *Ann. Otol. Rhinol. Lar.* **83**, 230–238.

TAKEMORI, S. & COHEN, B. (1974*a*). Visual suppression of vestibular nystagmus in rhesus monkeys. *Brain Res.* **72**, 203–212.

TAKEMORI, S. & COHEN, B. (1974*b*). Loss of visual suppression of vestibular nystagmus after flocculus lesions. *Brain Res.* **72**, 213–224.

TER BRAAK, J. W. G. (1936). Untersuchungen über optokinetischen Nystagmus. *Archs néerl. Physiol.* **21**, 309–376.

UEMURA, T. & COHEN, B. (1973). Effects of vestibular nuclei lesions on vestibulo-ocular reflexes and posture in monkeys. *Acta oto-lar.* suppl. 315, 1–71.

UEMURA, T. & COHEN, B. (1975). Loss of optokinetic after-nystagmus (OKAN) after dorsal medullary reticular formation (MedRF) lesions. Proceed. of the Barany Society. *Int. J. Equil. Res.* suppl. 1, 101–105.

WAESPE, W. & HENN, V. (1976). Behavior of secondary vestibular units during optoleinetic nystagmus and after-nystagmus in alert monkeys. *Pflügers Arch.* **362**, R50.

YASUI, S. (1974). Nystagmus generation, oculomotor tracking and visual motion perception. Ph.D. Thesis, Department of Aeronautics and Astronautics, Massachusetts Institute of Technology.

YASUI, S. & YOUNG, L. R. (1975). Perceived visual motion as effective stimulus to pursuit eye movement system. *Science, N.Y.* **190**, 906–908.

YOUNG, L. R. (1971). Pursuit eye tracking movements. In *The Control of Eye Movements*, ed. BACH-Y-RITA, P., COLLINS, C. & HYDE, J. E., pp. 429–446. New York: Academic.

ZADEH, L. & DESOER, C. A. (1963). *Linear System Theory: The State Space Approach.* New York: McGraw Hill.

ZEE, D., YEE, R. D. & ROBINSON, D. A. (1976). Optokinetic responses in labyrinthine-defective human beings. *Brain Res.* **113**, 423–428.